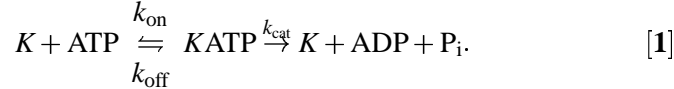


Supporting Text

Simple Model for Kinesin

To show the validity of the Monte Carlo approach, we will show that it reproduces the previous experimental results obtained for kinesin (1), which can also be calculated analytically by using the Michaelis-Menten expression. Kinesin moves processively toward the plus end of a microtubule by taking 8-nm steps. The dependence of the velocity V on ATP is successfully reproduced by Michaelis-Menten kinetics that describes binding of a kinesin head, denoted by K , to an ATP molecule and the subsequent hydrolysis



k_{on} (k_{off}) are rate constants for binding (unbinding) of an ATP by the kinesin head. k_{cat} is the rate constant of catalysis or hydrolysis of ATP, and P_i is the phosphate ion. We have included the fact that experimentally, reversal of hydrolysis is negligible (2).

This leads to the Michaelis-Menten expression for the velocity V of the motor on a microtubule (MT)

$$V = \frac{V_{\text{max}}[\text{ATP}]}{[\text{ATP}] + K_m}. \quad [2]$$

$V_{\text{max}} = k_{\text{cat}}d\varepsilon(F)$ is the maximum kinesin velocity at saturating ATP, $d = 8$ nm is the step size, F is the load, and $[\text{ATP}]$ is the ATP concentration. $\varepsilon(F)$ is the load-dependent coupling efficiency between ATP hydrolysis and mechanical stepping. It is independent of ATP concentration. We choose $\varepsilon(F) = 1 - (F/F_o)^2$ in order to interpolate between 100% efficiency at no load and zero at the stalling force F_o . $K_m = (k_{\text{cat}} + k_{\text{off}})/k_{\text{on}}$ is the Michaelis-Menten constant.

One interesting feature of molecular motors is that there is a link between the applied load and their enzymatic properties. We can model this load dependence by including it in the rate constants. Kinesin experiments indicate that increasing load results in a decrease in V_{max} and an increase in K_m . The decrease in V_{max} is accounted for by the coupling efficiency, which allows us to take k_{cat} to be load independent. To account for the observed increase in K_m , we need either k_{on} to decrease or k_{off} to increase (or both) with increasing load. We choose $k_{\text{off}} = k_{\text{off}}^o \exp[F\delta/k_B T]$ where k_B is the Boltzmann's constant, $T = 300$ K is the temperature in Kelvin, $k_{\text{off}}^o = 55$ s⁻¹, and $\delta = 1.6$ nm.

We now describe the Monte Carlo method and how it can be used to simulate the kinetic cycle of a molecular motor. Monte Carlo is an approach to computer simulations in which an event A occurs with a certain probability P_A where $0 \leq P_A \leq 1$. In practice, during each time step, a random number x is generated with uniform probability between 0 and 1. If $x \leq P_A$, event A occurs; if $x > P_A$, event A does not occur. Monte Carlo is also able to handle cases where multiple outcomes are possible. For example, suppose there are three possibilities so that either event A can occur with probability P_A or event B can occur with probability P_B or neither occurs. Then, if $x \leq P_A$, A occurs; if $P_A < x \leq (P_A + P_B)$, B occurs; and if $(P_A + P_B) < x \leq 1$, neither occurs.

We model a kinesin head by having it be in one of two states s . Either an ATP molecule is bound to the head ($s = 1$) or ATP is not bound ($s = 0$). The kinetic cycle corresponds to binding ATP (going from $s = 0$ to $s = 1$ with probability $P_{\text{on}} = k_{\text{on}}[\text{ATP}]\Delta t$), followed by hydrolysis of ATP and release of ADP and P_i (transition from $s = 1$ to $s = 0$ with probability $P_{\text{cat}} = k_{\text{cat}}\Delta t$), and taking a step of size $d = 8$ nm with probability $\varepsilon(F)$. It is also possible that if an ATP is bound to the kinesin head, it is released without being hydrolyzed with probability $P_{\text{off}} = k_{\text{off}}\Delta t$. We set the length of a time step $\Delta t = 10^{-5}$ sec. As Figs. 7 and 8 show, our Monte Carlo simulation reproduces the experimentally observed relationship between motor velocity and ATP concentration, as well as the effect of applied load on the velocity. (More details of our Monte Carlo algorithm are available below.) A

further test of consistency is provided by the fact that the results obtained by the Monte Carlo simulation match very well the analytical results of Eq. 2.

The kinetic scheme indicated above and implemented in the Monte Carlo simulation does not explicitly include interactions between the two heads. This is certainly incorrect, as we know that in order for a motor such as kinesin to be processive, there must be precise coupling of the enzymatic cycles for the two heads. In fact, this simplification is common (3, 4), and is resolved when we realize that in the intact dimeric motor, one step of the enzymatic cycle (e.g., P_i release) likely requires strain induced from the other head (5-7). While we have not put such strain into our model, the rate constant k_{cat} implicitly reflects the other head's activity—if the motor was really functioning as a monomer, this rate constant would be very different from the one we use. We use such a simplification for dynein as well, where we choose a single rate constant for the multiple processes of release of ADP and P_i (see below), at least one of which is presumably dependent on the activity of the second head.

Monte Carlo Algorithm for Kinesin Model

We will now give more details as to how we used a Monte Carlo algorithm to simulate the chemical kinetic cycle of kinesin. Let us describe a kinesin head by a two-state variable $s = 0, 1$ with $s = 1$ representing kinesin binding an ATP molecule and $s = 0$ representing kinesin without ATP bound.

1. *Initial condition:* Start at $t = 0$ with $s = 0$ and $x = 0$, where x is the position of the motor on the MT.
2. *Binding/Unbinding ATP:* At any given time t , switch the value of s with probability $P_{\text{on}} = k_{\text{on}}[\text{ATP}]\Delta t$ or $P_{\text{off}} = k_{\text{off}}\Delta t$, depending on whether the current value of s is 0 or 1. Here Δt sets the basic time step in the simulation. Δt must be sufficiently smaller than the typical time scale over which the fastest process in the mechano-chemical cycle occurs. For example, at saturating ATP levels and moderate loads, the binding of ATP is the fastest process. Given the ATP on rate for kinesin ($k_{\text{on}} = 2 \times 10^6 \text{ M}^{-1}\cdot\text{s}^{-1}$), ATP binding will take typically 10^{-4} s for an ATP concentration of 5 mM. This is why we have taken $\Delta t = 10^{-5}$ s.
3. *Hydrolysis and Step:* If $s = 1$, hydrolysis takes place with probability $P_{\text{cat}} = k_{\text{cat}}\Delta t$. After hydrolysis $s \rightarrow 0$ and $x \rightarrow x + d$ with probability $\epsilon(F)$.
4. $t \rightarrow t + \Delta t$ and the process repeats.

Details of Dynein Model

Monte Carlo Algorithm

1. *Binding/Unbinding ATP:* Just as for kinesin, we begin with $s = 0$ and $x = 0$ at time $t = 0$, where s denotes the number of ATP bound to the dynein head and x is the position of the motor on the MT. At any given time t , we either add an ATP to a vacant binding site or remove the one that is already bound with the probability given by the the appropriate k_{on} or k_{off} rates, depending on the current value of s , the number of ATP molecules already bound. At any given time ATP binding is updated as follows:
 - (a) If $s = 0$, set $s = 1$ with probability $p_{\text{on}}^1 = k_{\text{on}}^1[\text{ATP}]\Delta t$ (bind site 1).
 - (b) If $s = 1$, set $s = 0$ with probability $p_{\text{off}}^1 = k_{\text{off}}^1\Delta t$ (unbind site 1) or set $s = 2$ with probability $p_{\text{on}}^2 = k_{\text{on}}^2[\text{ATP}]\Delta t$ (bind a secondary site).

- (c) If $s = 2$, set $s = 1$ with probability $p_{\text{off}}^2 = k_{\text{off}}^2 \Delta t$ (unbind a secondary site) or set $s = 3$ with probability $p_{\text{on}}^3 = k_{\text{on}}^3 [\text{ATP}] \Delta t$ (bind another secondary site).
- (d) If $s = 3$, set $s = 2$ with probability $p_{\text{off}}^3 = k_{\text{off}}^3 \Delta t$ (unbind a secondary site) or set $s = 4$ with probability $p_{\text{on}}^4 = k_{\text{on}}^4 [\text{ATP}] \Delta t$ (bind third secondary site).

There is a subtle change in the scheme of binding/unbinding when ADP at site 1 has been released upon taking a step following hydrolysis. In this case the first addition of ATP (after hydrolysis) is done with probability p_{on}^1 . The removal or subsequent addition of ATP, however, remains same as described above. To be specific, suppose site 1 is empty. Then the whole scheme can be described as

- (a) If $s = 0$, set $s = 1$ with probability $p_{\text{on}}^1 = k_{\text{on}}^1 [\text{ATP}] \Delta t$ (bind site 1).
- (b) If $s = 1$, set $s = 0$ with probability $p_{\text{off}}^2 = k_{\text{off}}^2 \Delta t$ (unbind a secondary site) or set $s = 2$ with probability $p_{\text{on}}^2 = k_{\text{on}}^2 [\text{ATP}] \Delta t$ (bind site 1).
- (c) If $s = 2$, set $s = 1$ with probability $p_{\text{off}}^3 = k_{\text{off}}^3 \Delta t$ (unbind one of the two ATPs at secondary sites) or set $s = 3$ with probability $p_{\text{on}}^3 = k_{\text{on}}^3 [\text{ATP}] \Delta t$ (bind site 1).
- (d) If $s = 3$, set $s = 2$ with probability $p_{\text{off}}^4 = k_{\text{off}}^4 \Delta t$ (unbind third secondary site) or set $s = 4$ with probability $p_{\text{on}}^4 = k_{\text{on}}^4 [\text{ATP}] \Delta t$ (bind site 1).

We assume that the on-rates for secondary sites, k_{on}^{2-4} , depend on load as

$$k_{\text{on}}^{2-4} = k_{\text{on}}^{2-4}(F = 0) \exp\left(\frac{F d_o}{k_B T}\right), \quad [3]$$

where d_o is an adjustable parameter with units of length. The exponential Boltzmann factor accounts for the increase in the ATP binding affinities of additional sites when the motor is under load. We assume that all other on-rates and off-rates are independent of load.

2. *Hydrolysis/Taking step*: When site 1 has an ATP bound, then it can undergo hydrolysis with probability $p_{\text{cat}} = k_{\text{cat}} \Delta t$. After hydrolysis, either the hydrolysis can reverse with probability p_{syn} or the motor can translocate to a new position on the MT with a step size depending on the number of ATP bound to secondary sites.

- (a) If $s \geq 1$, *hydrolyze* with probability p_{cat} .
- (b) If hydrolysis has occurred, *reverse* hydrolysis can occur with probability p_{syn} .
- (c) If reversal occurs, s and x remain unchanged. If there is no reversal, a step occurs ($x \rightarrow x + d$), and ADP is released from site 1 with $s \rightarrow s - 1$.

Here k_{cat} , which is an effective rate for hydrolysis, can depend on the number of ATP bound to the secondary binding sites – first, through the ATPase rate being dependent on whether or not a secondary site is bound, and second, through the step size and load-dependent Boltzmann factor. We take

$$k_{\text{cat}} = A(s) k_{\text{cat}}^o \exp(-\alpha F d(s) / k_B T), \quad [4]$$

where $d(s)$ depends on the number of ATP bound to secondary sites. $d(s)$ equals the size of the step that may be taken. Here $A(s)$ gives the reduction factor in the catalytic rate when a secondary site is not bound and α is the load distribution factor for the hydrolysis (4, 8). The reversal of hydrolysis also depends on load as

$$p_{\text{syn}} = p_{\text{syn}}^0 \exp(\beta F d(s) / k_B T), \quad [5]$$

where β is the load distribution factor for the reversal of hydrolysis. As suggested in refs. 4 and 8, $\alpha + \beta = 1$.

3. $t \rightarrow t + \Delta t$ and the process is repeated.

Experimental Constraints

As inputs to any model, we need numerical values for various rate constants. For guidance into the values of these constants, we use experimental data as available. As axonemal dynein has been more extensively studied biochemically, many of the approximate rate constants we use reflect these measurements. First, the binding affinity of ATP at site 1 lies in the range of $10^4 - 10^5 \text{ M}^{-1}$ (9, 10). Second, the binding affinity of ATP at a secondary site is likely be an order of magnitude lower than site 1, and the binding of ATP at additional secondary sites could be still lower (9). Further, we need to choose rate constants such that the motor moves at the correct speed. It is also known that at saturating ATP levels (11), cytoplasmic dynein moves with an average speed of $\approx 700 \text{ nm/s}$ and around ATP concentrations of 1 mM , the motor attains 80% of its maximum velocity. While the step sizes at very low levels of ATP are mostly 32 and 24 nm, the step sizes even at saturating levels of ATP in the absence of any load are not all 8 nm (12).

Actual Choice of Values

It turns out that these constraints are satisfied by the following choice (which is not unique): $k_{\text{on}}^1 = 4 \times 10^5 \text{ M}^{-1} \cdot \text{s}^{-1}$, $k_{\text{off}}^1 = 10 \text{ s}^{-1}$, $k_{\text{on}}^2(0) = 4 \times 10^5 \text{ M}^{-1} \cdot \text{s}^{-1}$, $k_{\text{on}}^3(0) = k_{\text{on}}^2(0)/4$, $k_{\text{on}}^4(0) = k_{\text{on}}^2(0)/6$, $k_{\text{off}}^2 = k_{\text{off}}^3 = k_{\text{off}}^4 = 250 \text{ s}^{-1}$, $k_{\text{cat}}^0 = 55 \text{ s}^{-1}$.

To implement the effect on ATP hydrolysis at site 1 by ATP binding/hydrolysis at site 3, we use a prefactor $A(s)$ for the probability of ATP hydrolysis at site 1:

$$\begin{aligned} A(s) &= 1 && \text{for } s > 1 \\ &= \frac{1}{100} && \text{otherwise.} \end{aligned} \quad [6]$$

In the simulation the load on motor is given by the restoring force $F = k_{\text{trap}}x$ as it moves away from $x = 0$, the center of the trap. We take the trap stiffness $k_{\text{trap}} = 0.007 \text{ pN} \cdot \text{nm}^{-1}$ as in ref. 12. The simulations were done using $d_0 = 6 \text{ nm}$, $\alpha = 0.3$, $\beta = 0.7$ and $p_{\text{syn}} = 0.23$.

It is worth mentioning that the simulations use an ATP off-rate for k_{off}^2 that is somewhat higher than one might expect from the argument given above (see *Experimental Constraints*) concerning the relative binding affinities. It should be noted, however, that once a step is taken, the leading head becomes the trailing head, and ATP unbinding from the trailing head would increase the effective off-rate. In addition to ATP detachment, the secondary binding sites can lose ATP through hydrolysis (13). So we use an effective off-rate that reflects all of these pathways.

Alternative Choice of Values

The binding affinities do not uniquely constrain the values of the on-rates and off-rates. In some monoclonal antibody-antigen systems, the variation in the binding affinities are a reflection of the dissociation rates (14, 15). So we also tried values with k_{on}^i fixed for all i , and with all the load dependence and variation in the binding affinities being reflected in the off-rates. The binding affinities were the same as before. The alternative values for the on-rates and off-rates that we tried are $k_{\text{on}}^1 = k_{\text{on}}^2(0) = k_{\text{on}}^3(0) = k_{\text{on}}^4(0) = 4 \times 10^5 \text{ M}^{-1} \cdot \text{s}^{-1}$, $k_{\text{off}}^1 = 10 \text{ s}^{-1}$,

$k_{\text{off}}^2 = 250 \text{ s}^{-1}$, $k_{\text{off}}^3 = 4 \times k_{\text{off}}^2$, $k_{\text{off}}^4 = 6 \times k_{\text{off}}^2$. The load dependence on the secondary sites was given by

$$k_{\text{off}}^{2-4} = k_{\text{off}}^{2-4}(0) \exp\left(-\frac{F d_o}{k_B T}\right), \quad [7]$$

where $d_o = 6 \text{ nm}$ as before. These alternative values did not change our original results if the error bars are taken into account.

References

1. Visscher, K., Schnitzer, M. & Block, S. M. (1999) *Nature* **400**, 184–189.
2. Hackney, D. D. (1996) *Annu. Rev. Physiol.* **58**, 731–750.
3. Schnitzer, M. J., Visscher, K. & Block, S. M. (2000) *Nat. Cell Biol.* **2**, 718–723.
4. Fisher, M. E. & Kolomeisky, A. B. (2001) *Proc. Natl. Acad. Sci. USA* **98**, 7748–7753.
5. Hancock, W. O. & Howard, J. (1998) *J. Cell Biol.* **140**, 1395–1405.
6. Uemura, S. & Ishiwata, S. (2003) *Nat. Struct. Biol.* **10**, 308–311.
7. Rosenfeld, S. S. & Sweeney, H. (2004) *J. Biol. Chem.* **279**, 40100–40111.
8. Fisher, M. E. & Kolomeisky, A. B. (1999) *Proc. Natl. Acad. Sci. USA* **96**, 6597–6602.
9. Mocz, G., Helms, M. K., Jameson, D. M. & Gibbons, I. R. (1998) *Biochemistry* **37**, 9862–9869.
10. Mocz, G. & Gibbons, I. R. (1996) *Biochemistry* **35**, 9204–9211.
11. King, S. J. & Schroer, T. A. (2000) *Nat. Cell Biol.* **2**, 20–24.
12. Mallik, R., Carter, B. C., Lex, S. A., King, S. J. & Gross, S. P. (2004) *Nature* **427**, 649–652.
13. Kon, T., Nishiura, M., Ohkura, R., Toyoshima, Y. Y. & Sutoh, K. (2004) *Biochemistry* **43**, 11266–11274.
14. Pecht, I. (1982) *Antigens* **6**, 1–68.
15. Kranz, D. M. & Voss, E. W. (1981) *Mol. Immun.* **18**, 889–898.

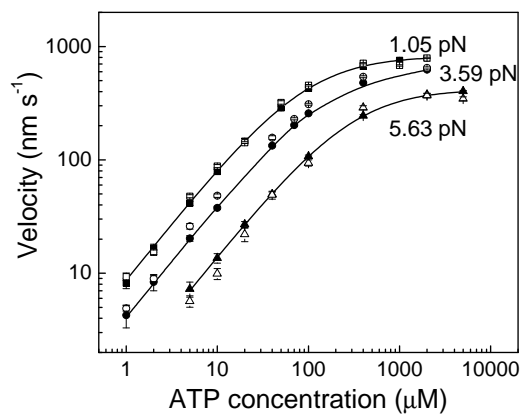


Figure 7: Average velocity vs. ATP concentration for kinesin. Open symbols are experiment (Ref. (1)), closed symbols are Monte Carlo, and the solid line represents the Michaelis-Menten formula (Eq. 2). For both Michaelis-Menten and Monte Carlo, we use $F_o = 8$ pN, $k_{on} = 2 \times 10^6$ M⁻¹·s⁻¹, and $k_{cat} = 105$ s⁻¹. These values apply for all the figures that involve kinesin in this paper. Error bars represent the standard deviation. Monte Carlo results average over 10 samples each having a duration of 50 s.

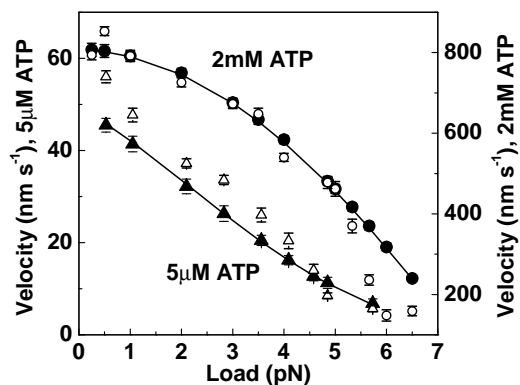


Figure 8: Velocity vs. load for kinesin at ATP concentrations of 5 μ M and 2 mM. Open symbols are experiment (Ref. (1)), closed symbols are Monte Carlo, and solid line represents the Michaelis-Menten formula (Eq. 2). Error bars calculated in the same way as in Fig. 7.